Electronic structure of disordered Au-Pd alloys studied by electron spectroscopies

Tschang-Uh Nahm,* Ranju Jung, Jae-Young Kim, W.-G. Park, and S.-J. Oh†
Department of Physics, Seoul National University, Seoul 151-742, Korea

J.-H. Park‡ and J. W. Allen
Department of Physics, University of Michigan, Ann Arbor, Michigan 48109-1120

S.-M. Chung
Department of Physics, Pohang University of Science and Technology, Pohang 790-784, Korea

Y. S. Lee and C. N. Whang
Department of Physics, Yonsei University, Seoul 120-749, Korea
(Received 20 January 1998; revised manuscript received 8 May 1998)

The occupied and unoccupied electronic structures of disordered Au_xPd_{1-x} alloys are studied by valence-band photoemission, bremsstrahlung isochromat spectroscopy (BIS), and x-ray absorption near-edge spectroscopy (XANES). The occupied partial spectral weights (PSW's) of Au $5d$ and Pd $4d$ states are obtained from the valence-band photoemission spectra using synchrotron radiation by taking the matrix-element effect into account. We use the Cooper minimum phenomenon of the Pd $4d$ states with the measured ratios of photoionization cross sections. The Pd $4d$ PSW's are found to form a virtual bound state in the Pd-diluted alloy but become broader as the Pd concentration increases due to the Pd $4d-$Pd $4d$ hybridization. On the other hand, Au $5d_{5/2}$ states show the common-band behavior due to the appreciable mixing with Pd $4d_{5/2}$ states, while Au $5d_{3/2}$ states retain their sharp structure and show the split-band behavior. These experimental PSW's of Au-Pd alloys are in good qualitative agreement with the results of recent self-consistent-field coherent-potential-approximation calculations. The comparison of the experimental Pd PSW of Au-Pd with those of other Pd–noble-metal alloys clearly shows that in noble-metal-rich alloys, the mixing of Pd $4d$ states with host d bands increases in the order of Ag-Pd, Au-Pd, Cu-Pd systems. This trend results in the split-band for Au-Pd and Ag-Pd in Pd diluted alloys, but gives the common band for Cu-Pd. The unoccupied Pd $4d$ states of disordered Au_xPd_{1-x} alloys obtained from BIS and XANES spectra show the gradual filling of Pd $4d$ states as the Au concentration is increased, but it is not completely filled even in the Pd-diluted alloy.
[S0163-1829(98)00339-7]

I. INTRODUCTION

There has been a great deal of effort to understand the electronic structure of disordered binary alloys. Especially, many experiments and calculations on binary alloys composed of transition metals and noble metals have been performed partly due to the interest in their catalytic behaviors and partly due to the intrinsic interest in the physics of the disordering effect. Among these, the electronic structures of disordered Pd alloys with noble metals have been interesting subjects because Pd partial densities of states (DOS's) are quite diverse among these systems. Also the noble-metal–Pd alloy systems have played an important role in developing theoretical computation methods. For example, Ag-Pd alloy system was the first one treated by self-consistent potentials within the Korringa-Kohn-Rostoker coherent-potential-approximation (KKR-CPA) scheme.[1] In this system the split-band behavior is observed, where the Ag $4d$ and Pd $4d$ states do not show strong mixing and are separate in energy. At first the band splitting between the Ag-related structure and the Pd-related structure had been overestimated with *ad hoc* potentials,[2] but this was brought into better agreement with experiment by employing *ab initio* potential obtained from self-consistent iterations.[3]

The self-consistent-field (SCF) KKR-CPA method was also used to calculate the electronic structure of disordered Cu-Pd alloys.[4] In this case, the agreement between theory and experiment turned out to be more difficult to achieve and a controversy was developed as to its origin. The main discrepancy between theory and experiment was that the calculated Pd partial DOS showed broader bandwidth and larger density of states for bonding states than photoemission experiments.[5–7] Some people argued that the local lattice relaxation effect around Pd sites was the cause of this discrepancy, and many theoretical works have tried to include the lattice relaxation effect to see if it can bring the theory into agreement with experiment. For example, tight-binding muffin-tin orbitals (TB-MTO) CPA (Ref. 8) calculation method was modified to treat the effect of the lattice relaxation approximately, imposing a relation between the changes in atomic-site volumes and the bulk moduli. The Pd partial DOS of Cu-rich Cu-Pd alloy predicted by this method had indeed reduced bandwidth,[8] but the agreement between theory and experiment was still not satisfactory. It turned out that the observed discrepancy stems mainly from the neglect of the matrix element (binding-energy dependence of photoionization cross section) and of the lifetime broadening in the interpretation of the photoemission spectra.[9,10]

Another Pd alloy system with noble metal, Au-Pd alloys, is the subject of investigation here. We believe this investigation is crucial to gain a comprehensive understanding of the band formation mechanism in Pd alloys, since the Au-Pd system is expected to be intermediate between Ag-Pd and Cu-Pd systems. The lattice spacing of the Au-Pd system is similar to that of the Ag-Pd system, which shows split-band behavior, while the relative energy position of the Au $5d$ and the Pd $4d$ band is similar to that of the Cu-Pd system, which shows overlapping bands. Hence the determination of the electronic structure of the Au-Pd alloy is very important in understanding band formation mechanism in noble-metal–Pd alloys as a whole.

Theoretically, the electronic structures of Au-Pd alloys have been calculated by KKR (Refs. 11–13) or TB-MTO (Ref. 14) CPA methods. The early non-SCF results[11] are now considered to be unreliable since they gave wrong values of the Pd $4d$ phase shifts and thus even the Pd-diluted alloys showed common-band behavior contrary to the later SCF results[12,14] (in Ref. 12, only the $Au_{70}Pd_{30}$ case was studied). The recent SCF TB-MTO calculation included the lattice relaxation effect approximately, but unfortunately neglected the spin-orbit splitting of Au $5d$ states, which is important for determining Au partial DOS of Pd-diluted alloys. A more recent fully relativistic SCF KKR-CPA result,[13] which includes the spin-orbit splitting of both components, is most reliable, and it predicts the existence of the Pd virtual bound state in Pd-diluted alloys in agreement with other SCF results. This calculation also predicts that as Au content increases, the $d_{3/2}$ states retain their split-band behavior but the $d_{5/2}$ states form a common band due to the appreciable mixing of the Au $5d_{5/2}$ and the Pd $4d_{5/2}$ states.

Experimentally the electronic structure of the Au-Pd system has been investigated before with x-ray photoemission spectroscopy (XPS),[5] ultraviolet photoemission spectroscopy (UPS),[6,12,15] and with synchrotron radiation.[16] For Pd-diluted alloys, the difference spectrum between the alloy and pure Au spectra[5,6] was interpreted as indicating the virtual bound state at the binding energy (designated as E_B henceforth) 1.6 eV. The early UPS work covering the whole composition range[15] argued the existence of both the Au and the Pd virtual bound states in their dilute limits. This interpretation however neglected the possibility of strong mixing between Pd and Au $d_{5/2}$ states as predicted by the later SCF band calculation. The recent synchrotron work by Blyth *et al.*[16] was most comprehensive, and it gave some insights into the overlapping structure of this system by comparing the spectra at photon energies 40 and 120 eV. However they only compared the d band peak energies between theory and experiment, and did not separate the spectra into the partial spectral weights (PSW's) of each component to compare in detail with band calculations. So it was not clear from this work alone how strongly Au $5d_{5/2}$ states mix with Pd $4d_{5/2}$ states in Pd-rich alloys, and how much Pd $4d$ states mix with Au $5d$ states in the Pd-diluted limit, which are crucial to answer the question whether or not a virtual bound state is formed.

In this paper, we obtain the occupied part of PSW's in Au-Pd alloys for the whole composition range. We make use of the cross-section change with photon energy, in particular the Cooper minimum phenomena of Pd $4d$ and Au $5d$ states, to extract PSW's of each constituent. We then compare them with theoretical calculations, and try to understand the change of the electronic structure as the composition is varied. And we also obtain the unoccupied Pd $4d$ states near the Fermi level E_F from bremsstrahlung isochromat spectroscopy (BIS) and x-ray absorption near-edge spectroscopy (XANES).

This paper is organized as follows. The experimental details are described in Sec. II. In Sec. III, we present the photoemission spectra of Au_xPd_{1-x} ($x=0.25$, 0.50, 0.75, 0.90) at different photon energies. In order to make use of the Cooper minimum phenomenon, the measured ratios of photoionization cross sections between Pd $4d$ and Au $5d$ states are also presented. Using these experimentally determined cross-section ratios as a function of photon energy, we then obtain the occupied part of the PSW's of alloys taking the matrix-element effect into consideration. We also show the unoccupied Pd $4d$ states near E_F measured by BIS and XANES experiments in Sec. III D. Then the comparison between our experimental results and the calculated PSW's is made in Sec. IV. Finally, we compare the Pd PSW's of the Au-Pd alloy with those of other noble-metal–Pd alloy systems in Sec. V to elucidate the band-formation mechanism and to understand quite different Pd partial DOS's depending on the noble metal. This paper concludes with a summary in Sec. VI.

II. EXPERIMENT

The polycrystalline alloy samples Au_xPd_{1-x} ($x=0.25$, 0.50, 0.75, 0.90) were prepared by arc melting of two constituents in an atmosphere of argon on water-cooled copper hearth. Since some of compositions have well-defined ordered structure (Au_3Pd and $AuPd_3$ have $L1_2$ structure below 850 °C and 780 °C),[17] all samples were annealed in the quartz ampoule at 950 °C for 48 h and then quenched in water to ensure homogeneity and disorder. The x-ray diffraction results with Cu $K\alpha$ lines confirmed homogeneous face-centered-cubic solid solutions.

The photoemission spectra were taken at National Synchrotron Light Source (NSLS) of Brookhaven National Laboratory in the U.S. and Pohang Light Source (PLS) in Korea. In NSLS we used beamline U4A equipped with 6-m/160° toroidal grating monochromator and the VSW HA100 concentric hemispherical analyzer with single channel electron detector. The photon energy ranged from 40 to 200 eV, and the total experimental resolution was maintained better than 0.3 eV full width at half maximum for photon energies below 160 eV. In PLS we used beamline 2B1 equipped with spherical grating monochromator and the VG CLAM2 analyzer with three channeltron detectors. The photon energy ranged from 100 to 250 eV to cover the Cooper minima of both Pd $4d$ and Au $5d$ states. All measurements were performed under a pressure in the low 10^{-10}-torr range.

Before the measurements, clean surfaces were obtained by sputtering with neon or argon ions with 1.0–2.0-keV kinetic energy for 20 min and by subsequent annealing at 200–240 °C for 20 min to cure damages induced by ion sputtering and obtain polycrystalline surfaces. The effect of sputtering was very clear for pure Pd or Pd-rich alloys; the states near the Fermi level were suppressed very strongly for

amorphous surfaces. So annealing the sample was inevitable despite the possibility of surface segregation, the effect of which turned out to be small for this system as will be seen below.

The BIS experiment was performed in an ultrahigh vacuum photoelectron spectrometer at Seoul National University manufactured by VSW. It consists of a quartz x-ray monochromator that is set at 1486.6 eV and CsI-coated photon detector. The incident electron beam current was in the range of 100–300 μA. The total resolution was $\sim$1.0 eV as measured by the width of the recorded step in the BIS spectrum at E_F. The BIS experiment was performed under a pressure in the high 10^{-10}-torr range. The sample surfaces were cleaned mainly by scraping with a diamond file. The cleanliness of the surface was checked by looking for the oxygen Auger peak and carbon 1s peak in the XPS experiment. Very little carbon and oxygen contaminations were detected.

Pd L_3-edge XANES spectra of the Au_xPd_{1-x} alloys were obtained at NSLS beamline X-19A. X-ray energy was varied using a Si(111) double-crystal monochromator that was detuned by $\sim$50% to minimize higher-order harmonics in the x-ray beam. The X19-A beamline was maintained under the ultrahigh vacuum by up to 10 mm-thick beryllium window located inside the hutch. To avoid thickness effect, the spectra were collected in the total electron yield mode.

III. RESULTS AND DISCUSSION

A. Photoemission data

Figure 1 shows photoemission spectra of the Au_xPd_{1-x} alloys along with Au and Pd pure metals taken at $h\nu = 70$ eV, where the calculated photoionization cross-section ratio[18] between Pd 4d and Au 5d states is 0.77. We can see that the spectral intensity at the Fermi level decreases appreciably for $Au_{50}Pd_{50}$ relative to pure Pd. This reduction of the Fermi-level spectral intensity is consistent with the reduction of the linear coefficient of the specific heat around 40% Pd.[13] It is to be noted that in pure Pd metal the prominent structure at $E_B\sim$2.5 and 4.5 eV predicted in the calculated DOS (thin line)[19] is barely visible in the experimental spectrum, and the overall shape of the photoemission spectrum is quite different from the calculated DOS due to the strong matrix-element effect.[9] Also, we can see that part of the Pd PSW in the Pd-diluted alloy lies at $E_B = 1.6$ eV by comparing the spectra of $Au_{90}Pd_{10}$ and pure Au.

Figure 2 shows the spectra taken at $h\nu = 120$ eV where Au 5d states are more emphasized (the calculated cross section of the Pd 4d is 0.3 times that of the Au 5d). While the lower binding structure in the Au spectrum, which consists mainly of the $5d_{5/2}$ states, is smeared out with decreasing Au content, the higher binding peak around $E_B \simeq 6$ eV, which consists mainly of the $d_{3/2}$ states, retains the sharp structure for all compositions.

The spectra of Figs. 1 and 2 do not show clearly the partial spectral weights of each d band because of the overlapping structure between Au 5d and Pd 4d states. For example, the amount of the Au PSW of $Au_{25}Pd_{75}$ near the Fermi level cannot be estimated from these raw spectra alone because the contribution of the Au 5d and the Pd 4d emissions may be comparable (the theoretical cross-section

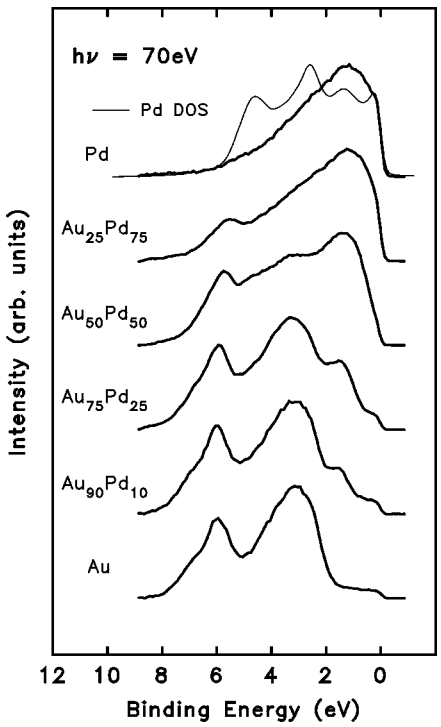

FIG. 1. Valence-band photoelectron spectra of Pd, $Au_{25}Pd_{75}$, $Au_{50}Pd_{50}$, $Au_{75}Pd_{25}$, $Au_{90}Pd_{10}$, and Au with photon energy $h\nu = 70$ eV from sputter-annealed surfaces, where the calculated cross-section ratio between Pd 4d and Au 5d states is 0.77. The inelastic background is removed and the analyzer transmission function is corrected assuming 1/E behavior. Also shown is the calculated Pd DOS from Ref. 19 (thin line).

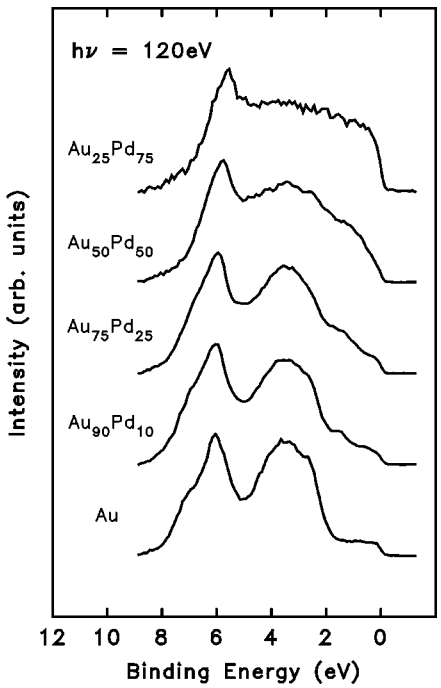

FIG. 2. Valence-band photoelectron spectra of $Au_{25}Pd_{75}$, $Au_{50}Pd_{50}$, $Au_{75}Pd_{25}$, $Au_{90}Pd_{10}$, and Au with photon energy $h\nu = 120$ eV where the calculated cross section of the Pd 4d is 0.3 times that of Au 5d states. Other details are the same as in Fig. 1.

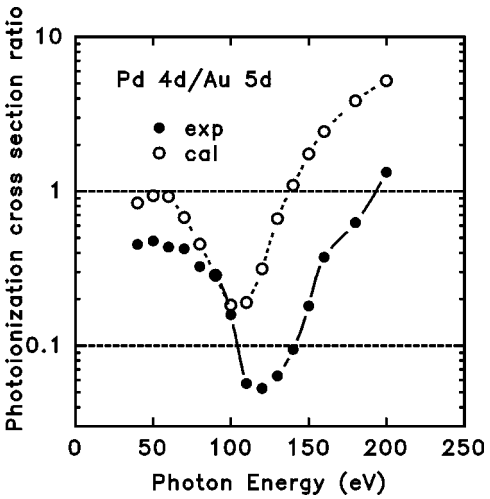

FIG. 3. Ratio of the photoionization cross section between Pd $4d$ and Au $5d$ states at $h\nu = 40-200$ eV, the experimental solid state (filled circles) and the calculated atomic cases (open circles) (Ref. 18). The Pd Cooper minimum makes a sharp dip at $h\nu \simeq 120$ eV.

ratio[18] is 1:0.3 and the composition ratio is 3:1). To determine PSW's quantitatively, therefore, we have to know the photoionization cross sections of each d state accurately, which is done in the next subsection.

B. Photoionization cross section of metals

The procedure determining the cross-section ratio of the valence bands of different elements has been fully discussed in Ref. 10. It is based on the fact that the intensity ratios of the valence-band photoemission spectra taken at different photon energies are proportional to their photoionization cross-section ratios. To fix the proportionality constant, the intensity ratio of core levels is used, since the core-level cross sections in the solid are not expected to change much from their atomic values. For the Au-Pd alloys, we used the Au $4d$ ($E_B = 336$ eV for $d_{5/2}$ peak) and the Pd $3d$ ($E_B = 335.1$ eV for $d_{5/2}$ peak) core levels, which have similar kinetic energies.

The results of these measurements are shown in Fig. 3 along with the atomic calculation.[18] The main differences between the theoretical and the experimental results are the shift of the Pd $4d$ Cooper minimum dip position and the smaller value of the experimental ratio throughout the whole photon-energy range, which can be attributed to the solid-state effect. We can see from this figure that the experimental cross-section ratio between Pd $4d$ and Au $5d$ states changes by more than a factor of 15 between $h\nu = 50$ and 200 eV, which is more than adequate to extract partial spectral weights of Pd $4d$ and Au $5d$ states separately as shown below.

C. Occupied partial spectral weights determined by photoelectron spectroscopy

We use the procedure discussed in detail in Ref. 10 to extract PSW's of the Au-Pd binary alloys. The underlying assumptions of this procedure are that the photoionization matrix-element effect can be treated independently of the

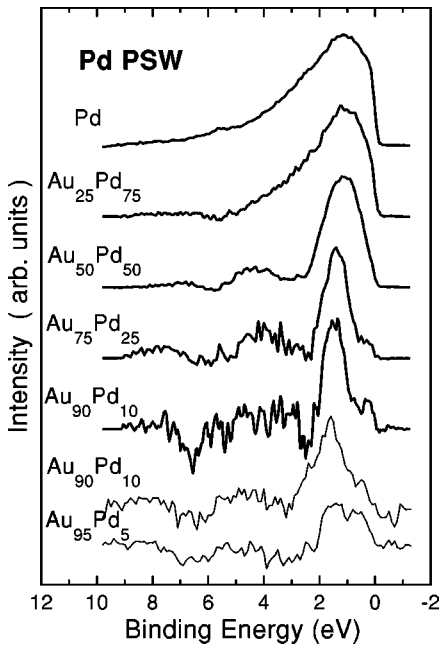

FIG. 4. Experimentally determined Pd partial spectral weights of Au_xPd_{1-x} alloys ($x = 0.0$, 0.25, 0.50, 0.75, and 0.90) at $h\nu = 70$ eV (thick line), and Pd-diluted alloys $Au_{90}Pd_{10}$, $Au_{95}Pd_5$ at $h\nu = 230$ eV (thin line).

total angular momentum ($j = 3/2$ and $5/2$) and that the matrix element of a constituent remains unchanged irrespective of the composition. Here we neglect contributions from s or p states because their cross sections are small, and use the spectra taken at $h\nu = 70$ and 120 eV to extract partial spectral weights of alloys for optimum resolution and statistics.

Since the measured cross-section ratio between Pd $4d$ states and Au $5d$ states is 0.053 at $h\nu = 120$ eV, the spectra at this photon energy can be regarded as the Au PSW's as a first step. Using the measured cross-section ratio and the divided spectrum representing the change in the matrix elements of pure Au with photon energy, the Pd PSW's at $h\nu = 70$ eV can then be obtained. By subtracting these Pd PSW's from the Au PSW's at $h\nu = 120$ eV after correcting for the matrix-element change, more correct Au PSW's can be obtained in turn. After several iterations, the results are converged to give the PSW's shown in Figs. 4 and 5.

In this analysis, we have assumed that the surface composition of alloys where photoelectrons are emitted is the same as in the bulk. It is well known that the surface composition of alloys may be different from the bulk because of the surface-segregation effect. However in the case of Au-Pd alloys, it has been determined that there is little surface-segregation effect in the sputtered surfaces.[20] Since we observed little difference between the photoemission spectra from the sputtered and the annealed surfaces in Au-rich Au-Pd alloys, and for Pd-rich alloys the total weights of the valence-band spectra from sputtered and annealed surfaces are about the same although they had slightly different shape, we used the bulk composition for all alloys in our analysis.

The top five curves in Fig. 4 show Pd PSW's of pure Pd and Au-Pd alloys at $h\nu = 70$ eV obtained by the above procedure. We can see that the Pd PSW of $Au_{90}Pd_{10}$ has dominant structure at $E_B < 2.5$ eV, although there may also be some small features in the region 3 eV $< E_B <$ 6 eV. The cen-

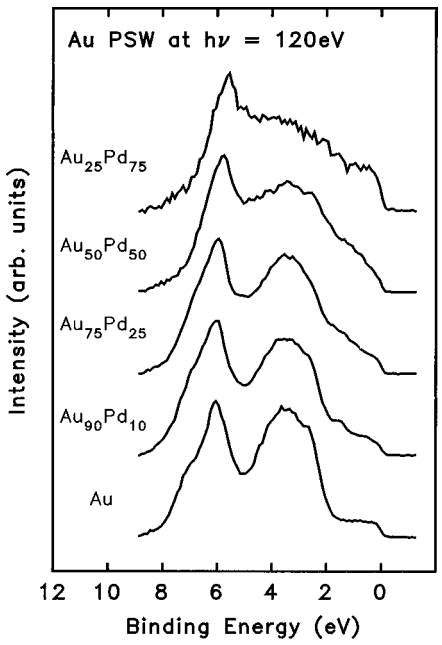

FIG. 5. Experimentally determined Au partial spectral weights of Au-Pd alloys at $h\nu = 120$ eV.

tral position of this dominant Pd PSW structure is at 1.6 eV, which is in agreement with the results obtained from the difference spectra for Pd-diluted alloys.[5,6] This structure suggests that the Pd impurity forms a virtual bound state in the Au host. We do not have clear explanation for the dips appearing at $E_B \simeq 2.5$ and 6.5 eV, but one possibility is they have resulted from the assumption of the composition-independent matrix element in alloys. These dips again appear in $Au_{75}Pd_{25}$, but we believe the structures at $E_B > 5$ eV are probably not real because the matrix element of the bonding type Pd $4d$ states is vanishingly small in this region.[10]

To confirm the existence of the virtual bound state in the Pd-diluted alloy and also to make sure that the above result does not depend on the photon energy used to extract PSW's, we took the valence-band spectra of $Au_{90}Pd_{10}$ and $Au_{95}Pd_5$ alloys at $h\nu = 130$ and 230 eV, which correspond to the Cooper minimum of Pd $4d$ and Au $5d$ states, respectively. The Pd partial spectral weights at $h\nu = 230$ eV for these Pd-diluted alloys are extracted by the same procedure as above, and the results are shown in the bottom two curves of Fig. 4 with thin lines. We can see that the Pd spectral weight of the $Au_{90}Pd_{10}$ alloy at $h\nu = 70$ eV (thick line, upper curve) and that $h\nu = 230$ eV (thin line, lower curve) are essentially the same if we take into account the difference of the experimental resolution. Furthermore, the Pd spectral weight of more diluted $Au_{95}Pd_5$ alloy also shows the virtual bound state. Hence we can conclude that Pd $4d$ state forms a virtual bound state in Pd-diluted Au-Pd alloys.

The evolution of Pd $4d$ states with the alloy composition shown in Fig. 4 can be interpreted as follows. We first note that the width of the Pd $4d$ states at $E_B < 2.5$ eV increases with the Au content, which is most likely the result of the Pd $4d$–Pd $4d$ hybridization. We also see that the Pd PSW's of $Au_{75}Pd_{25}$ and of $Au_{50}Pd_{50}$ have small structures at $E_B \simeq 4$ eV due to the Au $5d_{5/2}$–Pd $4d$ hybridization. The other spin-orbit component Au $5d_{3/2}$ states are little involved in this hybridization, since sharp structures around 6 eV due to the Au $5d_{3/2}$ states are not smeared out (see Fig. 5) and also there is no sign of the Pd spectral weight forming resonance with the Au $5d_{3/2}$ states. The Pd PSW of $Au_{25}Pd_{75}$ is very similar to the spectra of pure Pd, which implies the importance of the Pd $4d$–Pd $4d$ hybridization at this composition. Also, the Pd PSW at the Fermi level increases as the Pd content increases.

In Fig. 5, we present the Au PSW at $h\nu = 120$ eV. As the Au content is decreased, the $5d_{5/2}$-related structure at the lower binding energy smears out strongly due to the mixing with the Pd $4d$ states, but the $5d_{3/2}$-related structure at the higher binding energy retains its prominent peak which shifts toward the Fermi level by a small amount. For $Au_{25}Pd_{75}$, the Au $5d_{5/2}$ states most of which originally lie at $E_B > 2.5$ eV in pure Au spread out and have large spectral weight even near the Fermi level. This results from the strong hybridization with the Pd $4d$ bands in the Pd-rich alloys. This is anticipated because the Au atomic site in the Pd-rich alloys is compressed to fit the smaller nearest-neighbor distance in the alloy, in contrast to the Pd atomic site in the Au-rich alloys, which is dilated to accommodate larger nearest-neighbor distance.[21] As a result, the Au $5d_{5/2}$ states in the Au-diluted Au-Pd alloy experience very strong hybridization, while the Pd $4d$ states in the Pd-diluted Au-Pd alloy form virtual bound states.

The band formation in $Au_{25}Pd_{75}$ alloy as discussed above can be understood as follows. If there were no hybridization between Au and Pd states, the Au partial DOS would simply become narrow upon alloying because of the decrease of the similar states at nearest-neighbor sites.[22] However, the mixing with Pd $4d$ states would change Au $5d$ partial DOS's, and moreover its effect on the Au $5d_{3/2}$ state is expected to be quite different from that on the $5d_{5/2}$ states. The interactions between Pd $4d$ and Au $5d_{3/2}$ states, which are well separated from each other, mainly result in the band repulsion. This yields well-preserved sharp structure of the Au $5d_{3/2}$-related states. On the other hand, for the Au $5d_{5/2}$ states that lie inside the Pd $4d$ band, the strong hybridization with Pd $4d$ states leads to the strong band mixing as can be seen in Fig. 5. Therefore we can conclude that the Pd-rich Au-Pd alloy has common-band structure for the Au $5d_{5/2}$ states but shows split-band behavior for the Au $5d_{3/2}$ states.

D. Unoccupied partial spectral weights determined by BIS and XANES

To determine the unoccupied part of the spectral weights for this Au-Pd alloy system, we performed BIS and Pd L_3-edge XANES measurements. BIS spectra of Au_xPd_{1-x} alloys ($x = 0$, 0.05, 0.25, 0.50, 0.75, 0.90, 1.0) are shown in Fig. 6. The spectra clearly reveal the reduction of the unoccupied Pd $4d$ DOS at E_F as Au concentration is increased, which is consistent with the occupied valence-band photoemission spectra discussed above. These BIS spectra are normalized to have the same height at 7 eV above E_F, assuming that the intensity at this energy comes mostly from the background. This is reasonable because at that high energy neither Au nor Pd d states are expected to exist and the photoionization cross sections of Au $6s$ and Pd $5s$ states are negligibly small (smaller than those of Au $5d$ and Pd $4d$

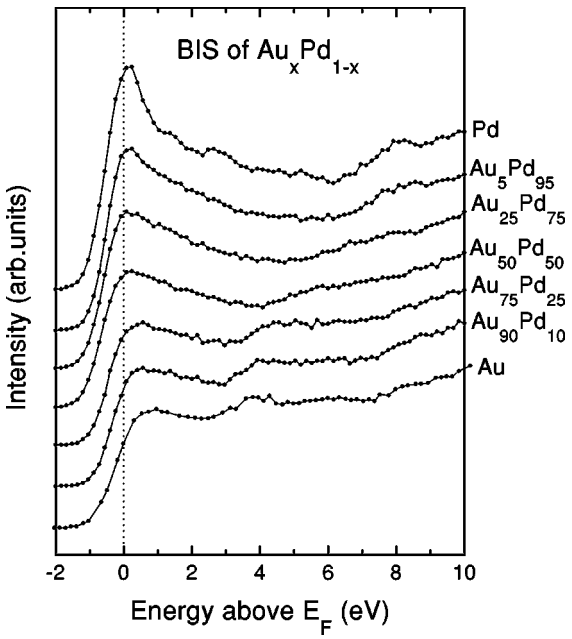

FIG. 6. BIS spectra of Au_xPd_{1-x} alloys ($x=0.0$, 0.05, 0.25, 0.50, 0.75, 0.90, and 1.0).

states by two orders of magnitude[18]), hence the contribution from the background should be dominant.

Here we are mostly interested in the unoccupied DOS of Pd $4d$ state above E_F. For this purpose, we use a simple subtraction procedure similar to that employed for the earlier BIS study of Cu-Pd alloys.[23] We first assume that partial DOS of Au s state does not change upon alloying. For Au-rich alloys this assumption is reasonable but for the Pd-rich alloys it may be somewhat inaccurate. But since the cross section of Pd $4d$ states is more than 50 times larger than that of Au $6s$,[18] a slight inaccuracy in the Au $6s$ DOS would not have serious consequences. With this assumption we obtain Pd partial BIS spectra of Au_xPd_{1-x} alloy by subtracting x fraction of pure Au BIS spectra from the alloy BIS spectra. In order to determine quantitatively the change of the number of unoccupied Pd $4d$ electronic states ($4d$ holes) by alloying, we then subtract the pure Ag BIS spectrum from this alloy Pd partial BIS spectra to get the weight of Pd $4d$ unoccupied states. This assumes that $5s$ bands for Ag and Pd are similar since Ag is next to Pd in the Periodic Table and the Ag $4d$ band is full. From the area of the resulting difference curve we can then obtain the weight of the unoccupied Pd $4d$ levels, which is converted to the number of Pd $4d$ holes n_d(BIS) in alloys by using the fact that the number of Pd $4d$ holes in pure Pd metal is 0.36 electron.[24] The result is shown in the second column of Table I. We can see from this table that the Pd $4d$ band is being gradually filled upon alloying with Au. However, even in $Au_{90}Pd_{10}$ where the Pd $4d$ hole number n_d is smallest, the Pd $4d$ band is not completely filled. This is consistent with the occupied part of the Pd partial spectral weights determined by the synchrotron radiation valence-band photoemission study discussed above.

Our BIS results are also consistent with the theoretical Pd partial DOS calculated with SCF TB-LMTO-CPA method.[14] This calculation predicts the reduction of the unoccupied Pd $4d$ DOS at E_F as Au concentration is increased, as observed in our BIS spectra. Also the calculation shows the Pd $4d$

TABLE I. The change of the number of Pd $4d$ holes in Au-Pd alloys as a function of the composition. The Pd $4d$-hole number n_d(BIS) is determined by BIS spectra and n_d(XANES) is obtained from XANES measurements. The experimental uncertainties for these numbers are estimated to be ± 0.01.

Pd (at. %)	n_d(BIS)	n_d(XANES)
100	0.36	0.36
95	0.32	0.33
75	0.25	0.30
50	0.18	0.26
25	0.10	
10	0.07	

unoccupied density of states above E_F becomes narrow and its centroid moves toward E_F as Pd is diluted, but still the Pd DOS extends down to the Fermi level even in the Pd dilute limit. This is consistent with our experimental observation that Pd $4d$ levels are filled but not completely as Pd is diluted.

Figure 7 shows the Pd L_3 XANES for various Au_xPd_{1-x} alloys ($x=0.00$, 0.05, 0.25, 0.50). These spectra have been background subtracted and normalized as follows. Since the total electron yield increases with the incident photon energy, the linear fit of the pre-edge region representing the absorption coefficient for photon energy lower than the absorption threshold is subtracted for each raw spectrum. The resulting curve is normalized by multiplying a factor that makes the continuum step the same height at a higher energy. The zero of the (relative) photon energy is assigned to the maximum point of each absorption spectrum. Figure 7 shows that the strength of the Pd white-line feature reduces dramatically compared to that of pure Pd with increasing Au concentration. The reduction of white-line strength indicates

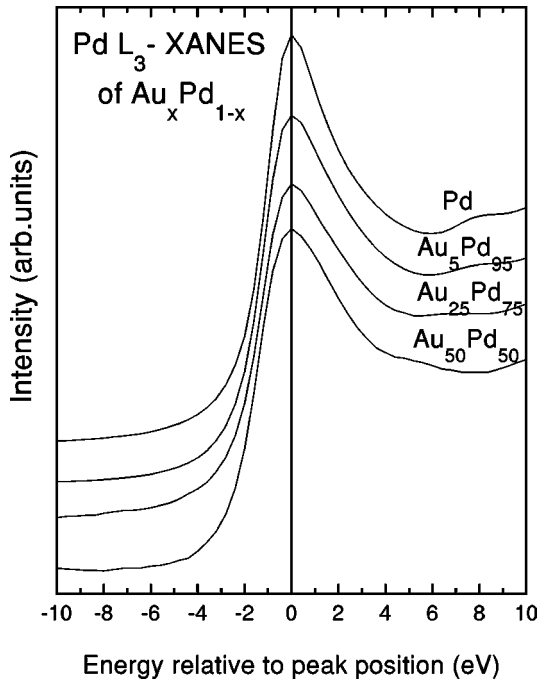

FIG. 7. Pd L_3 x-ray absorption near-edge spectra of Au_xPd_{1-x} alloys ($x=0.0$, 0.05, 0.25, and 0.50).

that the unoccupied density of d states projected onto the Pd atomic sphere is reduced upon alloy formation with Au. In order to calculate quantitatively the change of the number of Pd $4d$ holes, the white-line area related to the $2p \rightarrow 4d$ transition, which should directly measure the number of empty $4d$ holes, has been calculated as follows.

The white-line feature rides on top of the continuum step feature, hence this background continuum must be subtracted from the L_3 XANES spectra to estimate the white-line strength. For this purpose, we use the L_3 XANES spectrum of pure Ag metal since Ag has almost no d hole. We subtract the Ag XANES spectrum from each alloy Pd L_3 XANES spectrum after shifting the energy so that its inflection point aligns with the white-line maximum of the alloy Pd XANES measurement. The resulting difference curve is then integrated up to an energy 4.5 eV above zero, and this area is converted to the number of Pd d holes in the same way as in the analysis of BIS. The results thus obtained are written as the Pd $4d$-hole number n_d(XANES) in the third column of Table I. Comparing this with n_d(BIS) of the second column obtained from the BIS analysis, we find that these two numbers are in reasonable agreement.

IV. COMPARISON WITH BAND CALCULATIONS

There have been many CPA calculations for the electronic structure of Au-Pd alloys.[11–14] The early non-SCF calculation could not explain the experimental results due to incorrect potentials especially for the Pd diluted case.[11] The SCF TB-MTO-CPA calculation, which was scalar relativistic, was soon performed,[14] but unfortunately it did not include the spin-orbit splitting of the Au partial DOS. However, the Pd partial DOS should be described correctly because the Pd $4d$ states have small spin-orbit splitting. It is to be noted that this TB-MTO-CPA result also included the lattice relaxation effect approximately. More recently the fully relativistic SCF calculation was performed,[13] and this result is expected to be most reliable since it included spin-orbit interaction of both components. However, this calculation did not consider the lattice relaxation effect.

So we here compare the experimental Pd $4d$ PSW with the Pd partial DOS calculated by SCF KKR-CPA (Ref. 13) and SCF TB-MTO-CPA,[14] and in the case of Au $5d$ PSW with the Au partial DOS calculated by SCF KKR-CPA.[13] For comparison, we convolute theoretical partial DOS's with the Lorentzian curve to include the lifetime broadening effect by assuming the Fermi-liquid behavior. The Lorentzian half-width is assumed to increase quadratically from zero at E_F to 0.49 eV at $E_B = 7.0$ eV for Au, and 0.67 eV for Pd at $E_B = 5.6$ eV. These binding energies correspond to the bottom of d bands. In order to determine the photoionization matrix element, the pure metal photoemission spectra are divided by the convoluted DOS's. The theoretical PSW's are then obtained by multiplying the theoretical partial DOS's with this matrix element, which are further convoluted with the Gaussian curve to match the instrumental resolution of the experimental spectra at E_F. The results are shown in Figs. 8 and 9 for $Au_{75}Pd_{25}$, $Au_{50}Pd_{50}$, and $Au_{25}Pd_{75}$.

The structures in the theoretical Pd PSW's at $E_B < 2.5$ eV shown in Fig. 8 are due to the antibonding-type states while those at $E_B \simeq 4$ eV are due to the bonding type

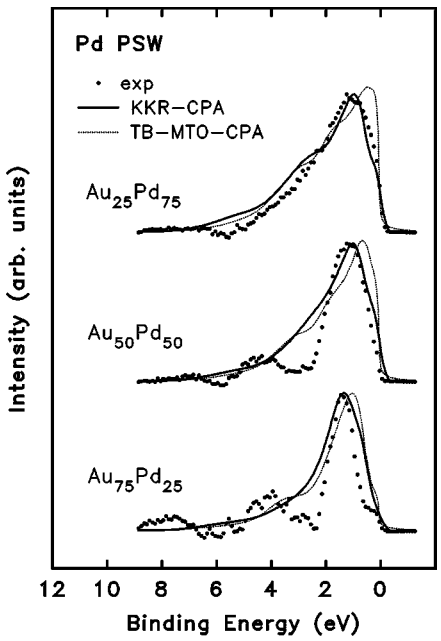

FIG. 8. Comparison of the experimental Pd partial spectral weights at $h\nu = 70$ eV (dots) with the theoretical Pd partial spectral weights of $Au_{25}Pd_{75}$, $Au_{50}Pd_{50}$, and $Au_{75}Pd_{25}$. The theoretical partial DOS's are from Ref. 13 (solid lines) and Ref. 14 (dashed lines).

from the hybridization with the Au $5d_{5/2}$ states. The main discrepancies between the theoretical curves and the experimental PSW's are the shifts of the states by 0.35–0.50 eV for TB-MTO-CPA calculation[14] and the presence of fairly strong spectral intensity at $E_B \simeq 3$ eV. The former can result from the inaccuracy of the theoretical Fermi-level position and the latter from the overestimation of the strength of the hybridization between the Pd $4d$ and the Au $5d$ states. However, the antibonding peak positions of the experimental and

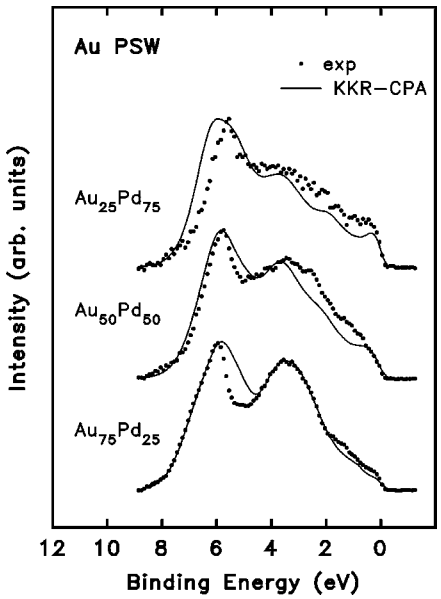

FIG. 9. Comparison of the experimental Au partial spectral weights at $h\nu = 120$ eV of $Au_{25}Pd_{75}$, $Au_{50}Pd_{50}$, and $Au_{75}Pd_{25}$ with theoretical PSW's. The experimental partial spectral weights are represented by dots and the theoretical partial spectral weights from Ref. 13 by lines.

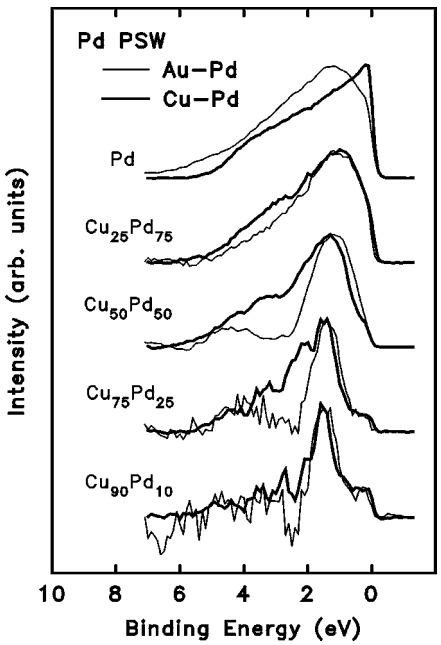

FIG. 10. Comparison of the experimental Pd partial spectral weights of Cu-Pd alloys at $h\nu = 40.8$ eV (thick lines) with those of Au-Pd alloys at $h\nu = 70$ eV (thin lines). The Pd atomic concentrations are the same in both cases.

the KKR-CPA PSW's are in excellent agreement.

We show the comparison of the experimental and the theoretical Au PSW's in Fig. 9. The Au $5d_{3/2}$ peak of $Au_{75}Pd_{25}$ and $Au_{25}Pd_{75}$ shifts by -0.4 and 0.2 eV, respectively, but the overall structures and the spectral intensities at E_F are in good agreement between experiment and theory. In particular, the experimental data confirm the theoretical prediction that as Au content increases the $d_{3/2}$ states retain their split-band behavior while the $d_{5/2}$ states form common-band due to the appreciable mixing of the Au $5d_{5/2}$ and the Pd $4d_{5/2}$ states.

V. COMPARISON WITH OTHER NOBLE-METAL–Pd ALLOYS

Now we compare the Pd PSW's of Au-Pd alloys with those of other noble-metal–Pd alloys.[25] Due to the strong matrix-element effect, part of the bonding states of pure Pd is not observable with $h\nu \leqslant 70$ eV. This obscures the correct observation of high binding structures of the Pd partial DOS, and therefore we will only compare structures at $E_B \leqslant 4$ eV here.

The Pd PSW's of Cu-Pd alloys at $h\nu = 40.8$ eV, which have been reported in Ref. 10, are compared with those of Au-Pd alloys in Fig. 10. Although the Pd PSW of $Cu_{90}Pd_{10}$ has a sharp structure at $E_B \simeq 1.7$ eV, this cannot be regarded as an indication of the virtual bound state because we do not fully observe bonding states at this photon energy as discussed in detail in Ref. 10. This is also true for $Au_{90}Pd_{10}$, but the existence of the virtual bound state is almost certain in this Pd-diluted Au-Pd alloy because of the weak hybridization between the Au $5d$ and the Pd $4d$ states resulting from the dilated Pd atomic site in the Au host as discussed above. The difference in the strength of the hybridization between Pd $4d$ and noble metal d states is clearly visible in Pd 25% or 50% alloy spectra. In Au-Pd alloys, there are two well-resolved structures in the Pd PSW's, but in Cu-Pd alloys only widely spread structure is observed due to stronger hybridization. This leads to the common band for the Pd-diluted Cu-Pd alloy but a split-band behavior for the Pd-diluted Au-Pd alloy.

The comparison between the Pd-diluted Ag-Pd and Au-Pd alloys requires the consideration of the spin-orbit splitting.[6] The width of sharp structures composed of antibonding states is larger in Ag-Pd alloys as shown in Ref. 6. At first sight, this seems to suggest stronger interaction between the host d band and the impurity d states. But this difference in widths in fact results from the difference in the shapes of the host d bands as discussed in Ref. 6. The Pd impurity states in Ag lie on a flat part of the host DOS, but in Au on a steep part of the host d band where abrupt change in DOS occurs. This leads to a simple broadening in the Ag host, but strong deformation in the Au host leading to a sharp structure above the Au $5d$ band and mixed states with the Au $5d$ band. Consequently, the width of the virtual bound state in Pd-diluted noble metal alloys cannot give quantitative information about the strength of the hybridization with the host d bands.

For the Pd-rich alloys, the band of the Ag-Pd alloy is close to the split-band type,[3] because only small overlap between two partial d DOS's leads to the band repulsion and yields small amount of mixing. The Au $5d_{3/2}$ state of the Au-Pd alloys also experiences small amount of mixing, but the other spin-orbit component Au $5d_{5/2}$ state of the Pd-rich Au-Pd alloy forms a common band with the Pd-host band. For the Pd-rich Cu-Pd alloy, both Cu $3d_{3/2}$ and $3d_{5/2}$ states form common band with the Pd-host band, as shown in Ref. 10.

For the unoccupied part of the Pd PSW, we can compare that of Au-Pd alloys discussed above with the case of Cu-Pd alloys studied in Ref. 23. We find in both cases the gradual filling of the Pd $4d$ band upon alloying with noble metals, but the unoccupied $4d$ states of Pd atom are not completely filled even in the Pd-diluted alloys $Cu_{90}Pd_{10}$ and $Au_{90}Pd_{10}$. There is quite similarity in the behavior of unoccupied Pd $4d$ band between Au-Pd alloys and Cu-Pd alloys.

VI. CONCLUSION

In this work, we have shown soft x-ray valence-band photoemission, BIS, and XANES spectra of Au-Pd alloys. We obtained PSW's of each constituent using the experimentally determined photoionization cross-section ratio and taking the matrix-element effect into consideration. We then compared the experimental PSW's of Au-Pd alloys with the theoretical PSW's from SCF-CPA calculations. They were found to be in good agreement overall for the Au PSW's, but some discrepancies could be seen in the Pd PSW's, which may be due to the overestimation of the hybridization strength. The unoccupied d states of Pd were also obtained from both BIS and XANES spectra using a simple subtraction procedure. We found that the Pd $4d$ unoccupied DOS near E_F becomes narrow and its centroid moves toward E_F as Pd is diluted, which leads to the gradual filling of Pd $4d$ holes. These results are in good agreement with theoretical calculations.

We have pointed out the differences in the mechanism

involved in the band formation of various Pd alloys with noble metals from the experimental PSW or the theoretical partial DOS of these systems. In Ag-Pd alloys, the dominating factor throughout the whole composition range is the band repulsion that leads to the split bands. In Au-Pd alloys, strong hybridization leads to common-band for Au $5d_{5/2}$ states in the Au-diluted alloys, while weak hybridization leads to the Pd virtual bound state in the Pd diluted alloys. This behavior is believed to be due to the size difference between Pd and Au. For Cu-Pd alloys, common-band behavior is expected throughout the whole composition.

ACKNOWLEDGMENTS

This work was supported in part by the Ministry of Education, Korea through Grants Nos. BSRI-96-2416 and BSRI-96-2440, and the Korean Science and Engineering Foundation through Atomic-Scale Surface Science Research Center (ASSRC) at Yonsei University. The synchrotron photoemission data were obtained at National Synchrotron Light Source, Brookhaven National Laboratory, which is supported by the Department of Energy, Division of Materials Sciences and Division of Chemical Sciences, and at Pohang Light Source in Korea, which is supported by the Ministry of Science and Technology, Korea.

*Present address: Department of Applied Physics, Stanford University, Stanford, CA 94305.

†Author to whom all correspondence should be addressed.

‡Present address: NSLS, Brookhaven National Laboratory, Upton, New York 11973.

[1] G. M. Stocks and H. Winter, Z. Phys. B **46**, 95 (1982); H. Winter and G. M. Stocks, Phys. Rev. B **27**, 882 (1983).

[2] A. J. Pindor, W. M. Temmerman, B. L. Gyorffy, and G. M. Stocks, J. Phys. F **10**, 2617 (1980).

[3] H. Winter, P. J. Durham, and G. M. Stocks, J. Phys. F **14**, 1047 (1984).

[4] H. Winter, P. J. Durham, W. M. Temmerman, and G. M. Stocks, Phys. Rev. B **33**, 2370 (1986).

[5] S. Hüfner, G. K. Wertheim, and J. H. Wernick, Solid State Commun. **17**, 1585 (1975).

[6] D. van der Marel, J. A. Jullianus, and G. A. Sawatzky, Phys. Rev. B **32**, 6331 (1985).

[7] H. Wright, P. Weightman, P. T. Andrews, W. Folkerts, C. F. J. Flipse, G. A. Sawatzky, D. Norman, and H. Padmore, Phys. Rev. B **35**, 519 (1987).

[8] J. Kudrnovský and V. Drchal, Solid State Commun. **70**, 577 (1989); Phys. Rev. B **41**, 7515 (1990).

[9] T.-U. Nahm, M. Han, S.-J. Oh, J.-H. Park, J. W. Allen, and S.-M. Chung, Phys. Rev. Lett. **70**, 3663 (1993).

[10] T.-U. Nahm, M. Han, S.-J. Oh, J.-H. Park, J. W. Allen, and S.-M. Chung, Phys. Rev. B **51**, 8140 (1995).

[11] H. Müller, H. Kirchmayer, P. Weinberger, P. Marksteiner, and J. Redinger, Z. Phys. B **67**, 193 (1987); P. Weinberger, R. Dirl, A. M. Boring, A. Gonis, and A. J. Freeman, Phys. Rev. B **37**, 1383 (1988).

[12] E. Arola, C. J. Barnes, R. S. Rao, and A. Bansil, Phys. Rev. B **42**, 8820 (1990).

[13] P. Weinberger, L. Szunyogh, and B. I. Bennett, Phys. Rev. B **47**, 10 154 (1993); P. Weinberger, C. Blaas, B. I. Bennett, and A. M. Boring, *ibid.* **47**, 10 158 (1993).

[14] J. Kudrnovský and V. Drchal, Phys. Status Solidi B **148**, K23 (1988).

[15] J. A. Nicholson, J. D. Riley, R. C. G. Leckey, J. G. Jenkin, and J. Liesegang, J. Electron Spectrosc. Relat. Phenom. **3**, 207 (1974).

[16] R. I. R. Blyth, A. B. Andrews, A. J. Arko, J. J. Joyce, P. C. Canfield, B. I. Bennett, and P. Weinberger, Phys. Rev. B **49**, 16 149 (1994).

[17] *Binary Alloy Phase Diagrams Vol. 1*, edited by T. B. Massalski (American Society for Metals, Metals Park, OH, 1986).

[18] J. J. Yeh and I. Lindau, At. Data Nucl. Data Tables **32**, 1 (1979).

[19] N. E. Christensen, J. Phys. F **8**, L51 (1978).

[20] G. Betz, Surf. Sci. **92**, 283 (1980).

[21] N. Mousseau and M. F. Thorpe, Phys. Rev. B **45**, 2015 (1992).

[22] M. G. Mason, Phys. Rev. B **27**, 748 (1983).

[23] E.-J. Cho, S. Lee, S.-J. Oh, M. Han, Y. S. Lee, and C. N. Whang, Phys. Rev. B **52**, 16 443 (1995).

[24] J. C. Fuggle, F. U. Hillebrecht, R. Zeller, Z. Zolnierek, P. A. Bennett, and C. Freiburg, Phys. Rev. B **27**, 2145 (1982).

[25] S.-J. Oh and T.-U. Nahm, J. Electron Spectrosc. Relat. Phenom. **78**, 43 (1996).